Mapping of Steroids Binding to 17β-Hydroxysteroid Dehydrogenase Type 1 Using Monte Carlo Energy Minimization Reveals Alternative Binding Modes†

Jonathan Blanchet,‡ Sheng-Xiang Lin,‡ and Boris S. Zhorov*,§

CHUL Research Centre, Laval University, Quebec City, Quebec, Canada, and Department of Biochemistry and Biomedical Sciences, McMaster University, Hamilton, Ontario, Canada

Received November 21, 2004; Revised Manuscript Received February 10, 2005

ABSTRACT: Crystallographic studies of ligand−protein complexes reveal most preferable ligand binding modes, but do not show less populated modes that may contribute to measurable biochemical and biophysical characteristics of the complexes. In some cases, a ligand may bind a protein in essentially different modes. An example is 17β-hydroxysteroid dehydrogenase type 1 (17β-HSD1), a steroidogenic enzyme that catalyzes reduction of estrone to estradiol in gonadal and peripheral tissues. The enzyme exhibits a high specificity for estrogens which bind with their C17 atom in the proximity of the NADP(H) cofactor. 17β-HSD1 can also bind androgens, but in a reverse binding mode, in which the steroid C3 atom is the closest carbon atom to the cofactor. Here we map the interaction energy of estradiol and dihydrotestosterone binding to 17β-HSD1. Positions and orientations of the steroids in the ligand-binding tunnel were sampled systematically, and at each combination of these generalized coordinates, the energy was Monte Carlo minimized. The computed maps show energy minima corresponding to the X-ray structures and predict alternative binding modes, in particular, an upside-down orientation in which steroidal face α is exposed to protein residues that normally interact with face β. The methodology can be used for mapping ligand−receptor interactions in various systems, for example, in ion channels and G-protein-coupled receptors that bind elongated ligands in confined space between transmembrane helices.

Systematic computational analysis of ligand−protein interactions with the goal of predicting possible ligand−receptor complexes requires mapping the ligand−protein energy against positions and orientations of the ligand. In some cases, the low-energy positions and orientations may be essentially different, representing different ligand-binding modes. The search for various ligand-binding modes can provide valuable information about ligand−receptor interactions, which may help design ligands with increased activity and specificity. The data for various ligand-binding models can also be useful for planning mutational experiments that would help in understanding the role of individual residues in ligand binding.

Generally, three translational and three orientational degrees of freedom specify the position and orientation of a ligand at a protein. The internal degrees of freedom, including torsional and bond angles, also define the geometry of ligand−protein complexes. However, the prediction of the ligand conformation at the given binding site is usually a simpler problem than the prediction of the binding site and binding mode of the ligand. A systematic search of ligand−receptor complexes in the space of all the six degrees of freedom is computationally expensive. In many cases, the dimensionality of the search can be reduced. Thus, when an elongated ligand binds in a ligand-binding tunnel, energetically preferable ligand−receptor complexes can be searched in the space of two essential generalized coordinates, which specify translation of the ligand in the tunnel and rotation of the ligand around its long axis. Nonessential generalized coordinates, which include four remaining rigid-body degrees of freedom of the ligand and internal degrees of freedom of the ligand and receptor, can be energy-optimized for each combination of the essential generalized coordinates. The elongated ligands and tunnel-like receptor sites are seen in some water-soluble proteins. They are also typical for transmembrane proteins such as ion channels and G-protein-coupled receptors, which are targets for many important drugs. In this study, we introduce a computational protocol for mapping the ligand−receptor energy against the two essential generalized coordinates and apply this protocol for mapping interactions of 17β-hydroxysteroid dehydrogenase type 1 (17β-HSD1)[1] with estradiol and dihydrotestosterone.

17β-HSD1 was chosen for evaluating the predictive power of the approach for two reasons. First, essentially different binding modes of steroids in 17β-HSD1 are known from biochemical and crystallographic experiments. Second, 17β-HSD1 is a well-studied enzyme that catalyzes reduction of estrone to estradiol (E2), the most potent estrogen. The enzyme plays an important role in peripheral and gonadal

† This work was supported by the grants of the Canadian Institutes of Health Research (CIHR) to B.S.Z. and S.-X.L. B.S.Z. is a recipient of the CIHR Senior Investigator award.

* To whom correspondence should be addressed. Phone: (905) 525-9140, ext 22049. Fax: (905) 522-9033. E-mail: zhorov@mcmaster.ca.

‡ Laval University.

§ McMaster University.

[1] Abbreviations: 17β-HSD1, 17β-hydroxysteroid dehydrogenase type 1; DHEA, dehydroepiandrosterone; DHT, dihydrotestosterone; MCM, Monte Carlo-minimization; MD, molecular dynamics; E2, estradiol; PDB, Protein Data Bank.

10.1021/bi047553x CCC: $30.25
Published on Web 04/20/2005

Chart 1: Sequence of 17β-HSD1[a]

```
  1 ARTVVLITGC SSGIGLHLAV RLASDPSQSF KVYATLRDLK TQGRLWEAAR
 51 ALACPPGSLE TLQLDVRDSK SVAAARERVT EGRVDVLVCN AGLGLLGPLE
101 ALGEDAVASV LDVNVVGTVR MLQAFLPDMK RRGSGRVLVT GSVGGLMGLP
151 FNDVYCASKF ALEGLCESLA VLLLPFGVHL SLIECGPVHT AFMEKVLGSP
201 EEVLDRTDIH TFHRFYQYLA HSKQVFREAA QNPEEVAEVF LTALRAPKPT
251 LRYFTTERFL PLLRMRLDDP SGSNYVTAMH REVFG
```

[a] Residues of the double-shell model are shaded, and flexible residues are in bold. Residues providing the largest contributions of van der Waals energy to the ligand−receptor interactions are underlined. Residues capable of forming H-bonds with the steroids are double underlined.

tissues and is implicated in breast cancer proliferation (*1*−*3*). The X-ray structures are available for the apoenzyme (*4*), the complexes of the enzyme with various steroids (*5*−*7*), and ternary complexes of the enzyme with steroids and NAD(P)(H) cofactors (*8*−*11*). In 17β-HSD1, the catalytically active residues are Ser142, Tyr155, and Lys159. These residues belong to the Ser-$(X)_n$-Tyr-$(X)_3$-Lys motif, which is conserved in the family of short-chain dehydrogenases/reductases (*4*, *12*, *13*).

The substrate-binding site of 17β-HSD1 has a form of a tunnel formed by predominantly hydrophobic and aromatic residues that provide a major contribution to the binding energy (*5*). Ser142, Tyr155, His221, and Glu282 can form H-bonds with the polar groups of the substrate. The binding site is covered by a flexible loop (residues 187−200) whose geometry is poorly defined in the three-dimensional structures. The enzyme can bind NAD(H) and NADP(H) cofactors. NADPH binds more strongly, enabling substrate reduction in vivo (*9*, *14*). In vitro, the enzyme can catalyze the reduction and oxidation of estrogens, depending on the cofactor that is used (*15*). Kinetic studies have shown that the reaction is random and that both binary (enzyme−steroid and enzyme−cofactor) and ternary (enzyme−steroid−cofactor) complexes can be formed (*16*). The reaction is not rate-limited as substrate inhibition was observed only with high concentrations of estrone (*17*).

Estrogens bind to 17β-HSD1 with the C17 atom approaching the cofactor (*5*, *8*). 17β-HSD1 was also crystallized with equilin, dihydrotestosterone (DHT), dehydroepiandrosterone (DHEA), testosterone, and androstandione (*6*, *7*, *10*, *11*). Testosterone and androstandione bind 17β-HSD1 in a reverse mode with the C3 atom approaching the cofactor (*7*, *11*). Kinetic studies show that, depending on the cofactor that is used, the enzyme can catalyze either 17β oxidation of DHT to androstandione or 3β reduction to 3β,17β-androstanediol (*7*). Estrogens form more stable complexes with the enzyme than androgens, but the latter can bind in both normal and reverse modes (*6*, *7*, *11*).

Computations of the Monte Carlo-minimized (MCM) energy profiles of steroids pulled via the ligand-binding tunnel of 17β-HSD1 predicted energetically optimal complexes in agreement with the X-ray structures (*18*). These computations demonstrated that the side-chain conformations of the enzyme and orientations of the substrates vary substantially. However, the intensive search for various possible orientations of the steroids has not yet been performed. In this work, we map the MC-minimized energy against the translation and orientation of E2 and DHT in 17β-HSD1 (PDB entry 1A27). The maps were computed for both normal and reverse binding modes, which were observed experimentally (*7*, *11*). The maps predict a substantial mobility of the steroids in the ligand-binding tunnel and new ligand-binding modes. The predictions are consistent with the available experimental data and help us understand atomic-level mechanisms of the steroid−enzyme interactions.

METHODS

Calculations were performed using ZMM (www.zmmsoft.com) as described previously (*19*, *20*). The AMBER force field (*21*) was used with a cutoff distance of 8 Å and a shifting function (*22*). The conformational search was performed using the MCM protocol (*23*). Ligand positions and orientations as well as torsional angles of the protein were sampled randomly in the MCM protocol. After each sampling, all variable degrees of freedom, including bond angles of the ligands, were relaxed by energy minimization. The protein bond angles were kept rigid. Atomic coordinates were taken from the crystallographic structure of 17β-HSD1 complexes with E2 and $NADP^+$ [PDB entry 1A27 (*9*)]. This structure has been chosen because of its relatively high resolution and defined geometry of the flexible loop. WHAT_CHECK (*24*) was used to optimize the network of H-bonds in the crystal structure and to assign tautomeric forms for histidines. To reduce the computational time, a double-shell model of the enzyme was built (Chart 1) (*18*). The first shell included flexible residues, which have at least one atom within 6 Å of the steroid or cofactor in the crystal structure. The backbone and side-chain torsion angles of the flexible residues were varied during energy minimizations. The second shell included rigid residues, which do not belong to the first shell and have at least one atom within 10 Å of the steroid or cofactor. Residues that are far from E2 in the crystal structure but can interact with E2 on its way along the ligand-binding tunnel to the position seen in the crystal were also included in the double-shell model. The cofactor has not been included in the model due to reasons discussed in a later section.

The hydration energy was estimated using an implicit-solvent method (*25*). Titratable residues were considered in their ionized state except for histidines that were treated as neutral. Partial atomic charges in the substrates were calculated using the AM1 method in MOPAC (*26*). Electrostatic interactions were calculated using the distance-dependent dielectric.

Steroids have a flattened-ellipsoid shape, which is complementary to the elongated ligand-binding tunnel of 17β-HSD1. As stated in the introductory section, for such a system ligand−protein interactions can be mapped in the space of two essential generalized coordinates: the translation of the steroid in the tunnel and its rotation around the long axis. To impose a specific position and orientation of the ligand bound to the protein, the local system of coordinates of the ligand was introduced with the origin at atom C3, the *z* axis (the long axis of the ligand) drawn from C3 to C17, and

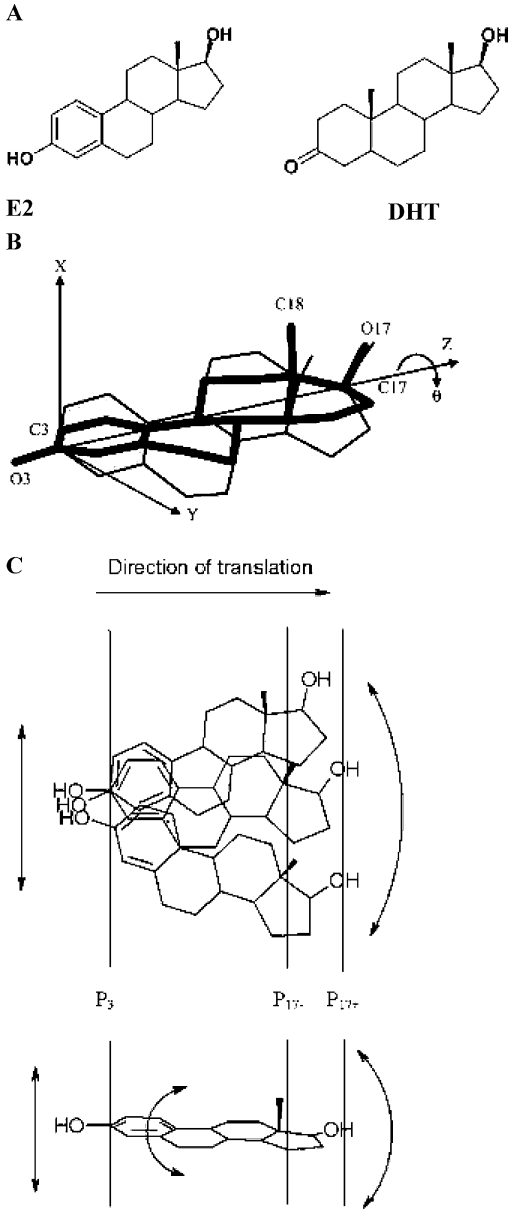

FIGURE 1: (A) Chemical formulas of E2 and DHT. Methyl groups protrude from face β, and the opposite face is designated α. (B) Definition of the ligand local system of coordinates. The *z* axis is drawn via C3 and C17. The $x-z$ plane is defined by atoms C3, C17, and C18. Euler angle θ specifies rotation of the ligand around the *z* axis. E2 is shown in two orientations: $\theta = 0°$ (bold) and $\theta = 30°$. (C) Constraining planes, which are used to translate steroids in the ligand-binding tunnel. Atom C3 is constrained to plane P_3 and atom C17 between planes P_{17-} and P_{17+}. Several orientations of E2, which are possible at a single translational position, are shown in the top panel. The bottom panel shows one of these orientations in the orthogonal projection. Straight and curved arrows indicate translations and rotations, respectively, of the steroid allowed without violating the atom-plane constraints. The distance of 1.8 Å between planes P_{17-} and P_{17+} allows the ligand's long axis to tilt up to 40° to the tunnel axis. This flexibility enables the steroid to follow the tunnel's curvature but prevents deviations of the ligand's long axis by more than 90° from the tunnel long axis. The latter is defined as the steroid long axis in the X-ray structure.

plane $x-z$ defined by atoms C18, C3, and C17 (Figure 1B). The coordinates of the origin specify the position of the ligand in the global system of coordinates. Euler angles φ and ψ specify the orientation of the *z* axis, and Euler angle θ specifies the rotation of the steroid around the *z* axis. To impose a target position of the steroid, atom C3 was restrained in plane P_3 and atom C17 between planes P_{17+} and P_{17-} (Figure 1C). The planes are normal to the C3−C17 axis in the X-ray structure. Translation of the steroid was achieved by simultaneous displacement of the three planes along the axis with a fixed step and MC-minimizing energy at each step. Displacement d_s of 0 corresponds to the crystal structure. Negative and positive values of d_s impose the ligand shift toward Glu282 and the cofactor binding site, respectively. The ligand was translated by varying d_s from −3 to 3 Å with a step of 1 Å.

Rotation of the ligand around the *z* axis was achieved by varying the generalized coordinate θ from −180 to 180° with a step of 15° and MC-minimizing the energy at each step. The steps for translation and rotation were chosen to achieve an acceptable map resolution for a reasonable computational cost. Test calculations of several local areas in the $d_s-\theta$ space with smaller steps did not reveal additional meaningful minima (data not shown). A θ value of 0° corresponds to the ligand orientation in the crystal. Positive increments of θ correspond to the clockwise rotation of the ligand viewed along the *z* axis. For each combination of d_s and θ, the energy was MC-minimized until one of the following criteria of convergence was achieved: 500 consecutive energy minimizations without the energy decrease or 4000 minimizations. Test calculations with more stringent criteria of convergence resulted in an energy decrease of ~1 kcal/mol, whereas shorter trajectories usually resulted in higher-energy structures. For the given substrate in the given binding mode, a total of 168 MCM trajectories were computed to map the energy against 7 translational and 24 rotational coordinates. The substrate−enzyme energy and its components were mapped by using a stand-alone module that extracted the energy characteristics from the stack of the 168 MC-minimized structures. A total of 672 MCM trajectories were computed for two ligands in two binding modes. Among these, 121 trajectories (18%) were terminated due to reaching the limit of 4000 minimizations; most of these trajectories occur in the high-energy zones of two-dimensional maps. The remaining 72% of trajectories were terminated due to reaching the limit of 500 consecutive minimizations without an energy decrease.

RESULTS AND DISCUSSION

Figure 2 shows the maps of the substrate−enzyme energy and its components. Each map has two low-energy zones. The first one covers the ligand positions from −2 to 2 Å and orientations from −45° to 60°, with the center corresponding to the X-ray structure of 17β-HSD1 with E2 (*5*, *9*). The second low-energy zone covers the ligand positions from −2 to 2 Å and orientations from 120° to −165°. Orientations from 80° to 120° and from −80° to −120° correspond to high-energy zones that separate the low-energy zones. In the energetically unfavorable orientations, the maximum-profile plane of the flattened ligand is approximately perpendicular to the maximum-profile plane of the flattened tunnel. This causes steric clashes between the steroid and the enzyme.

To discriminate between steroid−enzyme complexes, we named the ligand orientations in which atoms C17 and C3 approach the cofactor as the normal and reverse binding modes, respectively (Figure 3). The normal binding mode has been observed in many crystals (*5*, *6*, *8*, *10*). The reverse

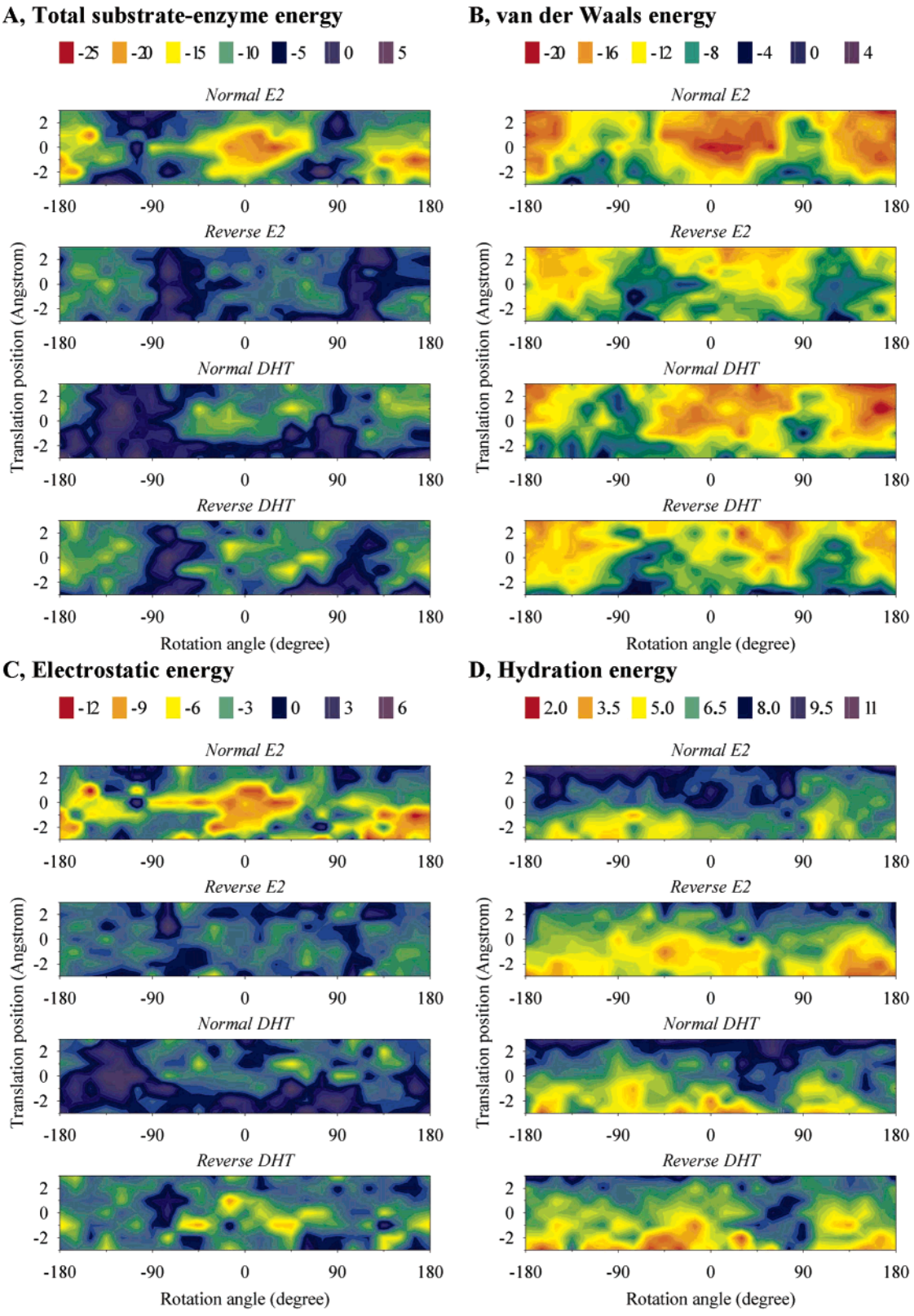

FIGURE 2: Maps of the steroid−enzyme energy (kilocalories per mole) and its components obtained from MC-minimized complexes of 17β-HSD1 with E2 and DHT. Each panel shows the energy in the normal and reverse binding modes. (A) Total steroid−enzyme energy. The lowest minima correspond to E2 in the normal binding mode. The reverse binding mode of DHT is more preferable than the normal one. All the maps have two low-energy zones where $\theta \approx 0°$ and $\theta \approx 180°$, which correspond to the regular and upside-down orientations, respectively. (B) van der Waals energy. The lowest energies for the normal mode are at $\theta \approx 0°$ and $\theta \approx 150°$ for most of the translational positions. The lowest energies for the reverse mode are at $\theta \approx 50°$ and $\theta \approx -150°$. In the reverse mode, E2 and DHT have optimal orientations from 30 to 50° at which the $C18H_3$ group fits between Leu149 and Val225 (*7*, *18*). (C) Electrostatic energy. Preferable interactions take place with E2 in the normal mode and DHT in the reverse mode. E2 binding in the reverse mode is electrostatically unfavorable. (D) Hydration energy. The energy increases as the steroids move deeper in the binding tunnel because of unfavorable dehydration of hydrophilic groups in both the enzyme and steroid. Both steroids are better hydrated in the reverse binding mode.

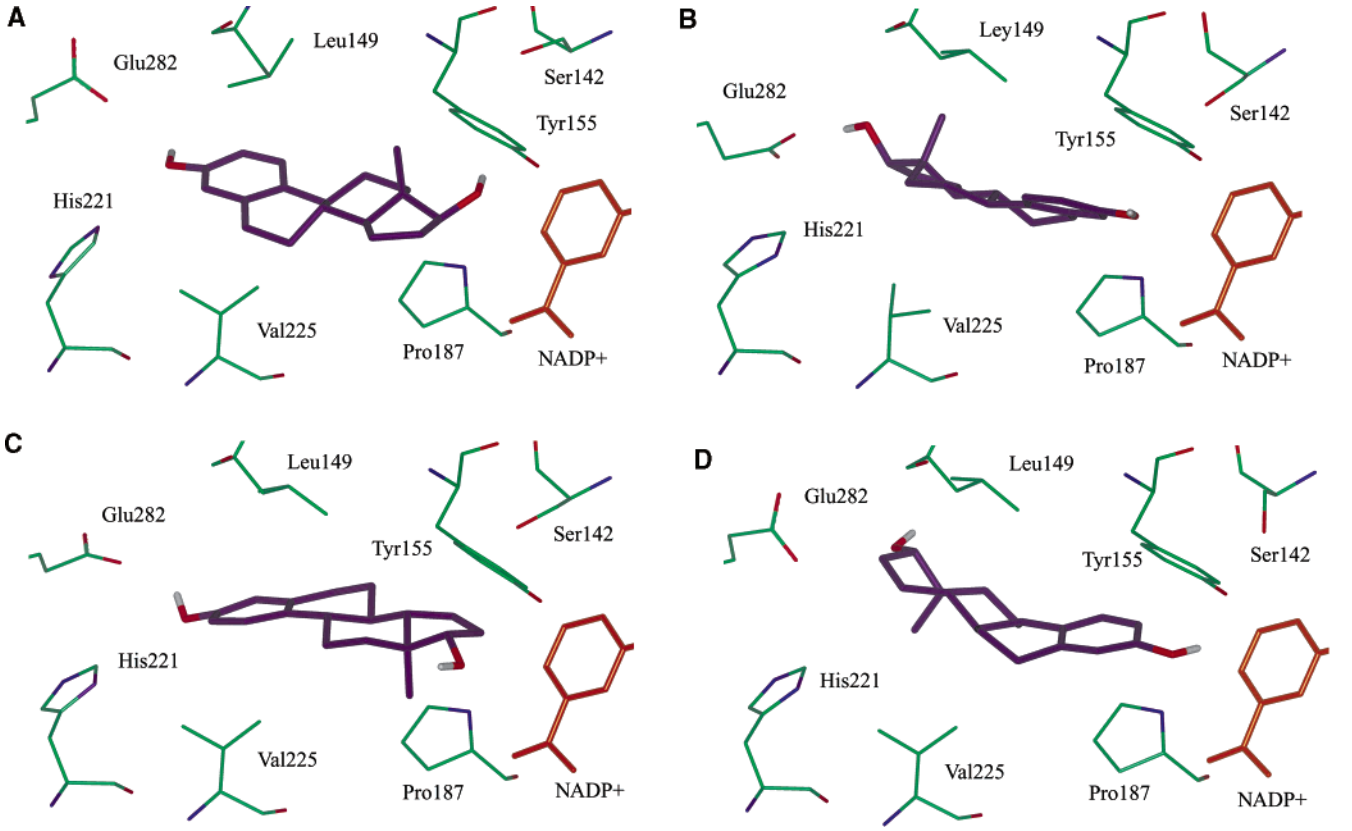

FIGURE 3: E2 in 17β-HSD1 in the normal (A and C) and reverse (B and D) binding modes with the regular (A and B) and upside-down (C and D) orientations. The cofactor nicotinamide moiety (orange sticks), which is not a part of the model, is drawn by using crystallographic coordinates. In the normal binding mode with the regular orientation (A), the O17 atom is well positioned to form H-bonds with Ser142 and Tyr155 and is close enough to the cofactor for hydride transfer. In the normal binding mode with the upside-down orientation (C), the position of the O17 atom is unfavorable for catalysis. In this orientation, O17 can form only a weak H-bond with Tyr155, while C17 is too far from the cofactor to allow hydride transfer. In the reverse binding mode (B and D), E2 would not participate in the catalytic reaction because O3 is not optimally disposed to form H-bonds and the phenyl ring is unsuitable for the reaction.

binding mode has been observed in the crystals with androgens (*7*, *11*). For the given binding mode, two low-energy orientations are possible. One orientation, named the regular one, corresponds to the X-ray structure of E2, in which steroidal face α is exposed to Val225 (Figure 3A,B). In another orientation, named the upside-down one, steroidal face β is exposed to Val225 (Figure 3C,D). The upside-down orientation was observed for androsterone and DHEA in DHEA-sulfotransferase (*27*, *28*), as well as for estradiol and C19 androgen metabolites in the sex hormone binding globulin (*29*). However, this orientation has not yet been observed experimentally in 17β-HSD1.

The lowest substrate−enzyme energy was observed for the normal binding mode and regular orientation of E2 (Figure 2A). The computed structure with $d_s = 0$ Å and $\theta = 0°$ coordinates is remarkably similar to the X-ray structure (Figure 4A). This fact is not trivial, since only essential generalized coordinates d_s and θ were imposed by constraints, while all other generalized coordinates were found by MC-minimizing the energy. The crystallographic structure has the lowest van der Waals energy (Figure 2B), but does not correspond to the lowest minimum of the total enzyme−substrate energy (Figure 2A). The crystallographic structure is entropically stabilized, since it is located in the middle of the largest low-energy zone. The latter also includes the second-best minimum at $d_s = 0$ Å and $\theta = 30°$ coordinates. The electrostatic energy is the major destabilizing factor of the crystallographic structure (Figure 2C). This energy term is least reliable in energy calculations because of variable dielectrics, unknown protonation states of ionizable residues, and unknown locations of counterions. The rather high electrostatic energy of the crystallographic structure may also reflect a possibility that the complex is in a near-transition state (*30*).

In the normal binding mode of E2, regular and upside-down orientations have minima almost equal in depth. However, the regular orientations occupy a much larger low-energy area (Figure 2A), suggesting that this orientation is more preferable entropically. In the regular orientation, the cofactor's hydride would attack atom C17 and Tyr155 would transfer its proton to the steroid's keto group (*4*, *8*, *31*). In the upside-down orientation, the carbonyl oxygen and C17 are far from their catalytically optimal positions (Figure 3). The reverse binding mode of E2 is unfavorable, having an energy ~10 kcal/mol higher than that of the normal mode. The upside-down orientation for the reverse binding mode is more preferable than the regular orientation.

In contrast to E2, the reverse binding mode of DHT is more favorable than the normal one. Regular and upside-down orientations of DHT are almost equal in energy (Figure 2A), which agrees with the pseudosymmetry of androgens (*7*). The major structural difference between these two steroids is that E2 has a flat aromatic A-ring with the hydroxyl group at C3, while the A-ring in DHT is saturated with a carbonyl group at C3 and a bulky C19 protruding at face β (Figure 1). The aromatic ring of E2 fits perfectly in

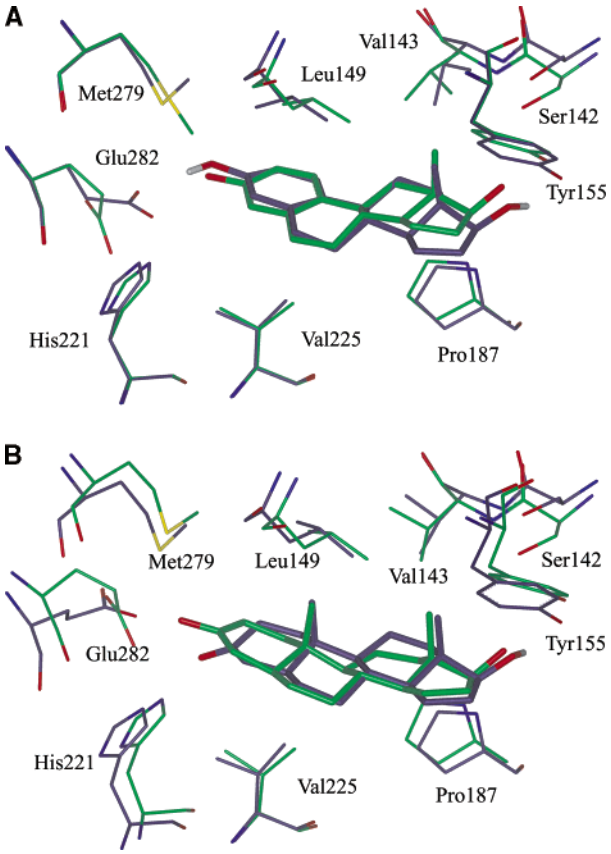

FIGURE 4: Modeled complexes of 17β-HSD1 with E2 and DHT (blue carbons) superimposed with the respective crystal structures (green carbons). In the modeled structures, $d_s = 0$ Å and $\theta = 0°$. (A) Modeled complex of 17β-HSD1 E2 vs the crystal structure [PDB entry 1A27 (*9*)]. In the model, the side chain of Glu282 moves toward the steroid hydroxyl O3-H, while displaced O17 does not form an H-bond with Ser142. (B) Modeled complex of 17β-HSD1 with DHT vs the crystal structure [PDB entry 1DHT (*6*)]. The O3 atom approaches Glu282 in the crystal, but His221 in the model. Side chains in the model and in the crystal are in similar conformations except for Glu282. Val143 has the same conformation in the model and in the crystal 1DHT (B), in spite of the different starting conformation of this residue used for modeling (A).

the flattened pocket between Leu149 and Val225, while C19H_3 of DHT does not fit there (*6*, *7*, *32*). In addition, hydroxyl O3-H of E2 can form an H-bond with Glu282, while carbonyl group O3 of DHT would repel from the negative charge at Glu282. In the normal binding mode, the crystallographic (*6*) and modeled structures of DHT have close coordinates of most atoms, except O3 (Figure 4B). As in the case of E2, the crystallographic orientation of DHT corresponds to a low-energy zone, but not to the apparent global minimum.

The van der Waals energy maps computed for the normal and reverse binding modes of both steroids are essentially different (Figure 2B). The lowest-energy zones are at $\theta = -30$ to 60° in the normal mode and $\theta = 0-90°$ in the reverse mode. Large low-energy zones are also seen for the upside-down orientations at $\theta \approx 180°$. In the X-ray structure of 17β-HSD1 with testosterone bound in the reverse mode (*7*), the steroid's orientation approximately corresponds to the energy minima at $\theta \approx 60°$, which are seen for the reverse modes of both E2 and DHT (Figure 2A). The minima are shifted from the $\theta \approx 0°$ orientation because in the reverse mode the steroid C18H_3 methyl group repulses Leu149 and Val225. In the normal mode, the C18H_3 group fits the binding site (not shown). E2 has better van der Waals interactions with the enzyme than DHT because the aromatic A-ring of E2 fits better in the ligand-binding pocket than the saturated ring of DHT does.

Hydrophobic and van der Waals interactions were proposed to play a major role in the binding of estrogens by 17β-HSD1 (*5*). The computed maps reveal the correlation between the total substrate−enzyme energy and its electrostatic component, suggesting that the latter plays an important role in substrate binding. Intermolecular H-bonds are generally formed in structures, which correspond to the minima of electrostatic energy. In the AMBER force field, most of the H-bonding energy appears under electrostatic interactions. The maps of electrostatic energy have deep and wide minima for E2 in the normal but not the reverse binding mode. In contrast, the reverse binding mode of DHT is stabilized by the preferable electrostatic interactions (Figure 2C), in agreement with the proposals that this mode is the most preferable for androgens (*7*, *11*). The electrostatic energy of DHT in the normal binding mode is poor. Glu282 plays an important role in the electrostatic discrimination of the binding modes. For E2 in the normal mode and DHT in the reverse mode, Glu282 usually contributes much more to the ligand−enzyme energy than other residues do. In contrast, Glu282 provides small or no contribution for the interaction energy of the steroids in the opposite modes (not shown). Indeed, hydroxyl O3-H of E2 in the reverse binding mode does not interact with Glu282, and the C3═O group of DHT in the normal mode is repulsed from the negatively charged Glu282.

The hydration energy of E2 and DHT in both normal and reverse binding modes increases with d_s (Figure 2D) since the hydrophilic groups in the steroid and enzyme are increasingly dehydrated as the ligand moves deeper into the protein. For both steroids, the hydration energy increases faster in the normal binding mode than in the reverse one. The highest hydration energy is seen at orientations from 40 to 100°, which correspond to the high-energy zones in maps of van der Waals energy. At these orientations, the plane of the steroid is normal to the plane of the binding pocket and some hydrophobic groups of both ligand and enzyme become available for an unfavorable hydration. The hydration of hydrophilic groups weakly depends on ligand orientation θ. Thus, van der Waals and electrostatic energy concertedly stabilize the experimentally observed positions and orientations of the steroid, while the hydration energy has both stabilizing and destabilizing components. The stabilizing component is preferable dehydration of hydrophobic groups in the steroid and the enzyme. The destabilizing component is nonpreferable dehydration of hydrophilic groups in the steroid and enzyme. Our calculations predict that the stabilizing component of the hydration energy is smaller than the destabilizing component. Without this compensation effect, steroids would bind too tightly with the enzyme.

Large dimensions of the low-energy zone that corresponds to the energetically preferable orientations of steroids in 17β-HSD1 (Figure 2A) indicate that the ligand-binding tunnel may be not as narrow as previously believed. When the ligand orientation deviates from that observed in the crystal, side chains move to retain stabilizing interactions with the

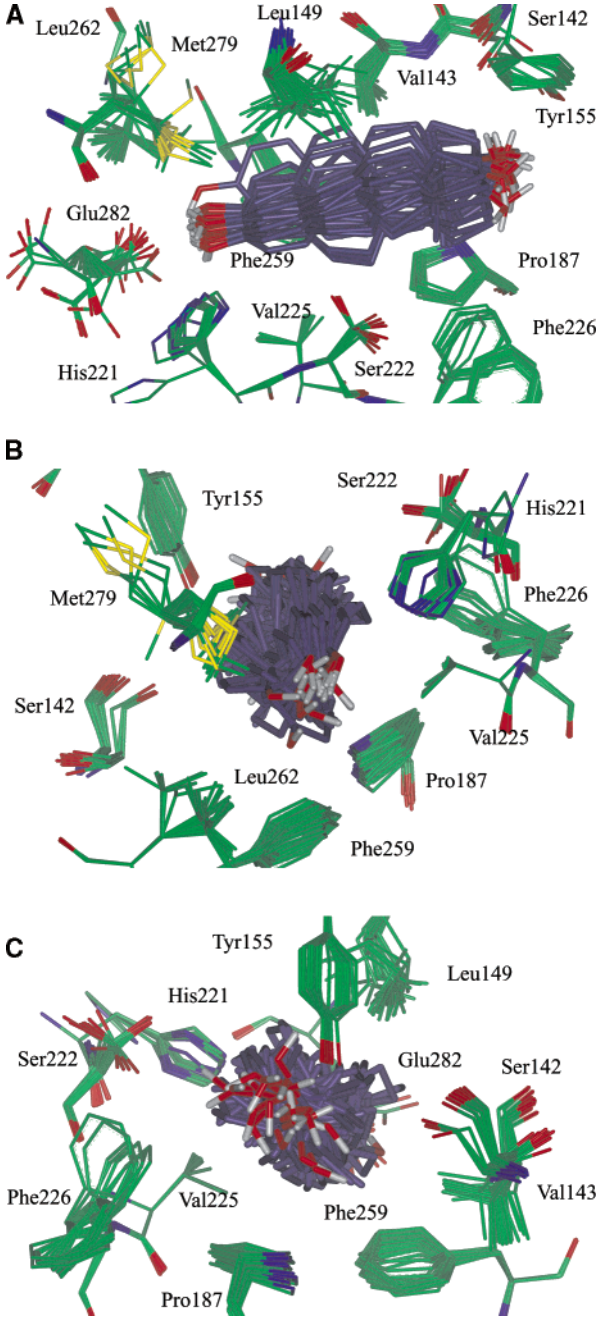

FIGURE 5: Superposition of different orientations of E2 at position $d_s = 0$ Å viewed normally to the C3−C17 rotational axis (A) and along the axis at the O3 atom (B) and the O17 atom (C). Side-chain conformations of the enzyme adapt to different orientations of the steroid. The catalytic reaction is hardly possible for most orientations because O17 cannot form H-bonds with catalytically active residues. However, some orientations may be interesting for the design of inhibitors.

ligand and/or to avoid destabilizing interactions (Figures 5 and 6). Side-chain torsion angles in residues that form direct contacts with the steroids may differ significantly between crystals. Remarkably, many of these torsion angles are observed in the models (Table 1). Glu282 is one of the most flexible residues, which adopts different conformations in the models (Figures 5 and 6). In crystal structures, this residue usually adopts two conformations, with the side chain pointing either toward the binding site (*5*, *6*) or toward the solvent (*8*, *9*). The crystallographic studies show the high *B*-factor of Glu282, indicating its high level of flexibility. Residues that weakly contribute to the interaction energy with the steroids, e.g., Cys156 and Tyr275, also are highly flexible in the crystal structures and in the models (not shown). For some residues, the models predict side-chain conformations which have not yet been observed in crystals.

Translational positions of steroids in 17β-HSD1, which have been observed in different crystals (*4*−*6*, *8*−*10*), are similar, suggesting that these positions are optimal for the catalytic process. The energy maps predict binding modes, positions, and orientations of E2 and DHT in agreement with the X-ray structures. They also predict new orientations that have not yet been observed experimentally. The maps demonstrate the plasticity of protein−ligand complexes and predict more than one binding mode, in agreement with observations that similar ligands can bind in different orientations in the same binding site (*33*, *34*). The analysis of different ligand-binding modes may be important for the design of inhibitors (*35*).

Figure 7 shows maps of E2 in 17β-HSD1 built with a single energy minimization at each combination of d_s and θ. The maps show a much higher energy for crystallographic complexes and smaller dimensions of the low-energy zones than corresponding maps computed by the MCM protocol (Figure 2A). The reason is that when the steroid is moved in the enzyme, the stabilizing steroid−enzyme contacts are destroyed and steric clashes appear. A subsequent single-energy minimization is unable to overcome energy barriers and find another energy minimum in which nonessential generalized coordinates, including side-chain torsion angles, would be more suitable for the new coordinates of the steroid. The comparison of maps in Figures 2A and 7 demonstrates the power of the MCM search versus the single-energy minimizations. It should be noted that the mapping of MC-minimized ligand−protein energy requires large computational resources. Therefore, the approach is currently not applicable for high-throughput studies aimed at identifying new leads of drugs. However, when the lead is known, the approach may provide valuable information for designing the lead analogues and planning mutational studies.

In this study, most computations were performed without the cofactor. The two-dimensional maps indicate that the substrate−enzyme interactions alone are sufficient to stabilize the experimentally observed substrate positions. Inclusion of the cofactor would limit the substrate translation to positions with positive d_s values where the substrate would collide with the cofactor. In the real system, such collisions result in REDOX reactions, the simulation of which requires quantum-chemical calculations. The comparison of the apoenzyme, enzyme−substrate complexes, and ternary complexes shows that the structures are rather similar. A few side chains are differently oriented in the ternary and binary complexes, but the conformational flexibility of these residues is usually reproduced in the models. The major changes are observed in the flexible loop, which has an open and poorly defined conformation in the absence of the cofactor. In the presence of the cofactor, the loop adopts a closed conformation and forms additional contacts with the substrate. The contacts hamper the substrate translation and rotation and thus are more suitable for evaluating the freedom of the substrate in the ternary complex. To predict the impact of the cofactor on substrate binding, we have built and MC-minimized models of the ternary complex with $NADP^+$ and

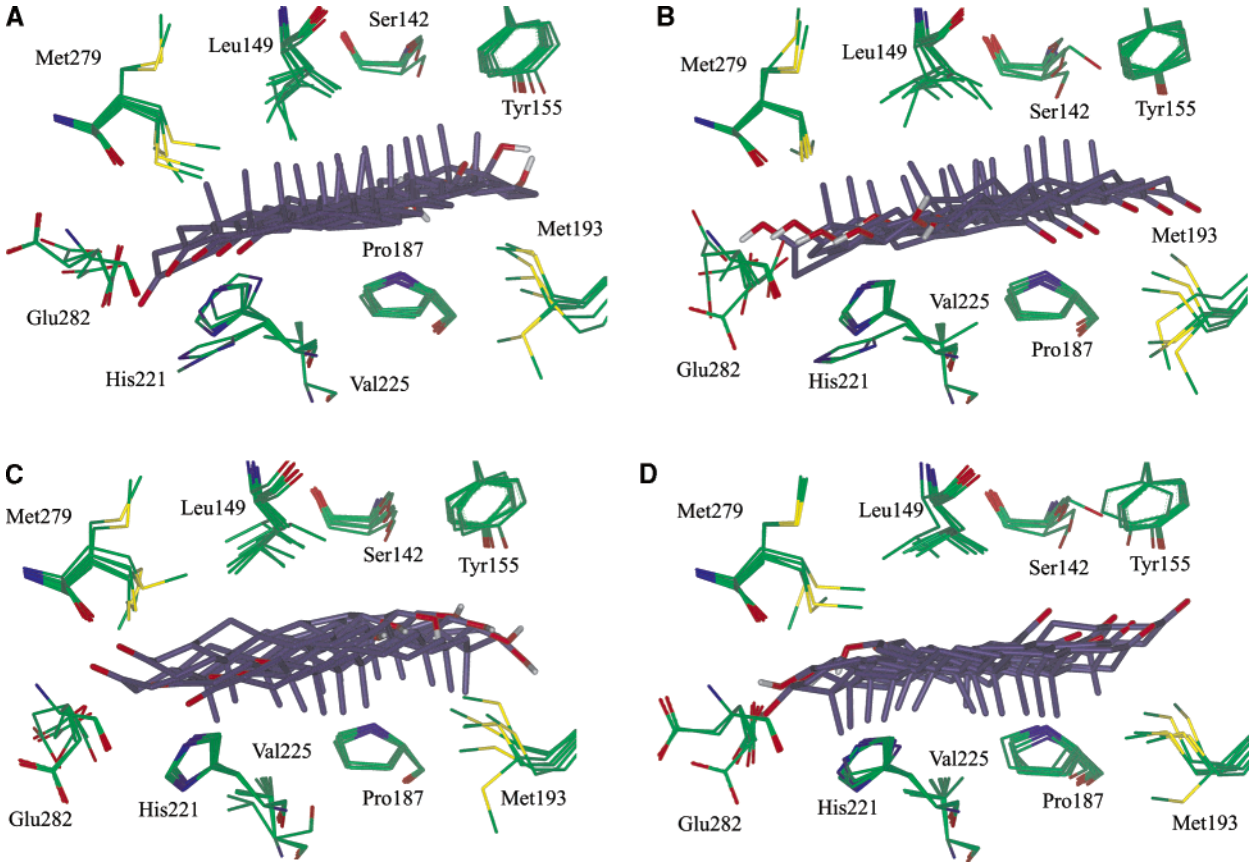

FIGURE 6: Superposition of several translational positions of DHT in the normal (A and C) and reverse (B and D) binding modes with the regular (A and B) and upside-down (C and D) orientations. Note that side chains of most residues move with the ligand.

Table 1: Crystallographic Conformations[a] in Side Chains of Residues that Form Direct Contacts with the Steroids[b]

residue	χ^1	χ^2	χ^3
Ser142	T		
Val143	G^- G T		
Leu149	G^-	T	
Tyr155	T	G	
Met193	T G^- **A**	T G G^- A	T A A^- **C** $\mathbf{G^-}$
Tyr218	T	G	
His221	T	G A^-	
Ser222	T G A **C**		
Val225	T A		
Phe226	T A^- $\mathbf{G^-}$	G	
Phe259	G^-	G^- A	
Leu262	T A^- G^-	G T	
Met279	T	G	G T A
Glu282	T A^-	T G A $\mathbf{G^-}$	

[a] The analyzed structures are described in refs *5*−*10*. T, C, G, G^-, A, and A^- denote torsion angles (conformation) of 180 ± 30° (*trans*), 0 ± 30° (*cis*), 60 ± 30° (*gauche*), −60 ± 30° (−*gauche*), 120 ± 30° (*anticlinal*), and −120 ± 30° (−*anticlinal*), respectively. Most of the experimental conformations have a match in at least one MC-minimized srtucture. Bold letters represent experimental conformations, which were not observed in the models. [b] Pro187 also forms direct contacts with the steroids. This residue is not included in the table since its five-membered ring has similar conformations in different crystals.

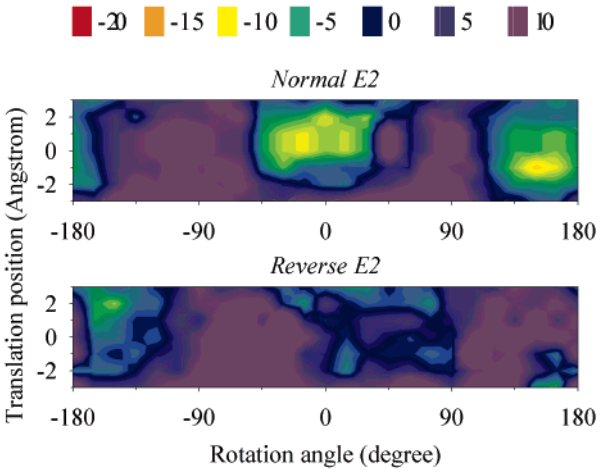

FIGURE 7: Two-dimensional maps of the interaction energy of E2 with 17β-HSD1 obtained after performing only a single-energy minimization at each combination of d_s and θ, which were sampled with the same step as in MC-minimized maps (Figure 2). Having high energy and small dimensions of the low-energy zones, the energy-minimized maps contrast with the MC-minimized maps.

E2 in the upside-down and reverse modes at position d_s = 0 Å (not shown). In the ternary complexes, E2 occupies the same position as in the cofactor-free models, although the side chains of some residues adopt different conformations. In the models with and without the cofactor, the same residues provide the largest contributions to the substrate binding energy. The difference in partitioned energy contributions between the models is less than 0.1 kcal/mol per residue. The cofactor contributed −0.74 kcal/mol to E2 binding in the normal mode, which is 2−3 times less than the contributions of Phe259 and Leu149.

In this work, we used the MCM method, which has been applied to find the global energy minimum of met-enkephalin, while molecular dynamics (MD) methods predicted higher-energy structures (*23*). Numerous applications of the MCM method have been reported, e.g., for ligand docking

(*36*, *37*) and simulation of large-scale conformational transitions in proteins (*38*). MD methods are realized in popular programs for molecular modeling and therefore are more often used in simulations of biomolecules. MD calculations were found to be more expensive computationally than Monte Carlo (*39*), but we are not aware of systematic comparisons of MD and MCM calculations for ligand−protein complexes. In the future, such a comparison would help us better understand advantages and disadvantages of both approaches.

In conclusion, mapping the MC-minimized energy in the space of position and orientation of steroids in 17β-HSD1 reveals the plasticity of the complexes. The maps correctly identify experimentally known steroid−enzyme complexes and predict alternative ligand-binding modes. The calculations show that electrostatic interactions are significant in determining the steroid−enzyme recognition. The computational protocol proposed in this work can be used for studies of complexes where elongated ligands bind in confined receptor sites. Ion channels and G-protein-coupled receptors exemplify such systems.

ACKNOWLEDGMENT

We thank Iva Bruhova for reading the manuscript and valuable comments and Dr. Jacques Lapointe for his help in drawing the two-dimensional maps.

REFERENCES

1. Martel, C., Rheaume, E., Takahashi, M., Trudel, C., Couet, J., Luu-The, V., Simard, J., and Labrie, F. (1992) Distribution of 17β-hydroxysteroid dehydrogenase gene expression and activity in rat and human tissues, *J. Steroid Biochem. Mol. Biol. 41*, 597−603.
2. Miyoshi, Y., Ando, A., Shiba, E., Taguchi, T., Tamaki, Y., and Noguchi, S. (2001) Involvement of up-regulation of 17β-hydroxysteroid dehydrogenase type 1 in maintenance of intratumoral high estradiol levels in postmenopausal breast cancers, *Int. J. Cancer 94*, 685−689.
3. Gunnarsson, C., Olsson, B. M., and Stal, O. (2001) Abnormal expression of 17β-hydroxysteroid dehydrogenases in breast cancer predicts late recurrence, *Cancer Res. 61*, 8448−8451.
4. Ghosh, D., Pletnev, V. Z., Zhu, D. W., Wawrzak, Z., Duax, W. L., Pangborn, W., Labrie, F., and Lin, S. X. (1995) Structure of human estrogenic 17β-hydroxysteroid dehydrogenase at 2.20 Å resolution, *Structure 3*, 503−513.
5. Azzi, A., Rehse, P. H., Zhu, D. W., Campbell, R. L., Labrie, F., and Lin, S. X. (1996) Crystal structure of human estrogenic 17β-hydroxysteroid dehydrogenase complexed with 17β-estradiol, *Nat. Struct. Biol. 3*, 665−668.
6. Han, Q., Campbell, R. L., Gangloff, A., Huang, Y. W., and Lin, S. X. (2000) Dehydroepiandrosterone and dihydrotestosterone recognition by human estrogenic 17β-hydroxysteroid dehydrogenase. C-18/c-19 steroid discrimination and enzyme-induced strain, *J. Biol. Chem. 275*, 1105−1111.
7. Gangloff, A., Shi, R., Nahoum, V., and Lin, S. X. (2003) Pseudosymmetry of C19 steroids, alternative binding orientations, and multispecificity in human estrogenic 17β-hydroxysteroid dehydrogenase, *FASEB J. 17*, 274−276.
8. Breton, R., Housset, D., Mazza, C., and Fontecilla-Camps, J. C. (1996) The structure of a complex of human 17β-hydroxysteroid dehydrogenase with estradiol and $NADP^+$ identifies two principal targets for the design of inhibitors, *Structure 4*, 905−915.
9. Mazza, C., Breton, R., Housset, D., and Fontecilla-Camps, J. C. (1998) Unusual charge stabilization of $NADP^+$ in 17β-hydroxysteroid dehydrogenase, *J. Biol. Chem. 273*, 8145−8152.
10. Sawicki, M. W., Erman, M., Puranen, T., Vihko, P., and Ghosh, D. (1999) Structure of the ternary complex of human 17β-hydroxysteroid dehydrogenase type 1 with 3-hydroxyestra-1,3,5,7-tetraen-17-one (equilin) and $NADP^+$, *Proc. Natl. Acad. Sci. U.S.A. 96*, 840−845.
11. Shi, R., and Lin, S. X. (2004) Cofactor hydrogen bonding onto the protein main chain is conserved in the short chain dehydrogenase/reductase family and contributes to nicotinamide orientation, *J. Biol. Chem. 279*, 16778−16785.
12. Oppermann, U. C., Filling, C., and Jornvall, H. (2001) Forms and functions of human SDR enzymes, *Chem.-Biol. Interact. 130−132*, 699−705.
13. Oppermann, U., Filling, C., Hult, M., Shafqat, N., Wu, X., Lindh, M., Shafqat, J., Nordling, E., Kallberg, Y., Persson, B., and Jornvall, H. (2003) Short-chain dehydrogenases/reductases (SDR): The 2002 update, *Chem.-Biol. Interact. 143−144*, 247−253.
14. Jin, J. Z., and Lin, S. X. (1999) Human estrogenic 17β-hydroxysteroid dehydrogenase: Predominance of estrone reduction and its induction by NADPH, *Biochem. Biophys. Res. Commun. 259*, 489−493.
15. Luu-The, V., Zhang, Y., Poirier, D., and Labrie, F. (1995) Characteristics of human types 1, 2 and 3 17β-hydroxysteroid dehydrogenase activities: Oxidation/reduction and inhibition, *J. Steroid Biochem. Mol. Biol. 55*, 581−587.
16. Betz, G. (1971) Reaction mechanism of 17beta-estradiol dehydrogenase determined by equilibrium rate exchange, *J. Biol. Chem. 246*, 2063−2068.
17. Gangloff, A., Garneau, A., Huang, Y. W., Yang, F., and Lin, S. X. (2001) Human oestrogenic 17beta-hydroxysteroid dehydrogenase specificity: enzyme regulation through an NADPH-dependent substrate inhibition towards the highly specific oestrone reduction, *Biochem. J. 356*, 269−276.
18. Zhorov, B. S., and Lin, S. X. (2000) Monte Carlo-minimized energy profile of estradiol in the ligand-binding tunnel of 17β-hydroxysteroid dehydrogenase: Atomic mechanisms of steroid recognition, *Proteins 38*, 414−427.
19. Zhorov, B. S. (1983) Vector method for calculating derivatives of the energy deformation of valence angles and torsion energy of complex molecules according to generalized coordinates, *J. Struct. Chem. 23*, 649−655.
20. Zhorov, B. S., and Bregestovski, P. D. (2000) Chloride channels of glycine and GABA receptors with blockers: Monte Carlo minimization and structure−activity relationships, *Biophys. J. 78*, 1786−1803.
21. Weiner, S. J., Kollman, P. A., Case, D. A., Singh, U. C., Ghio, C., Alagona, G., Profeta, S., Jr., and Weiner, P. K. (1984) A new force field for molecular mechanical simulation of nucleic acids and proteins, *J. Am. Chem. Soc. 106*, 765−784.
22. Brooks, C. L., Pettitt, B. M., and Karplus, M. (1985) Structural and energetic effects of truncating long ranged interactions in ionic and polar fluids, *J. Chem. Phys. 83*, 5897−5908.
23. Li, Z., and Scheraga, H. A. (1987) Monte Carlo-minimization approach to the multiple-minima problem in protein folding, *Proc. Natl. Acad. Sci. U.S.A. 84*, 6611−6615.
24. Hooft, R. W., Sander, C., and Vriend, G. (1996) Positioning hydrogen atoms by optimizing hydrogen-bond networks in protein structures, *Proteins 26*, 363−376.
25. Lazaridis, T., and Karplus, M. (1999) Effective energy function for proteins in solution, *Proteins 35*, 133−152.
26. Dewar, M. J. S., Zoebisch, E. G., Healy, E. F., and Stewart, J. J. P. (1985) AM1: A New General Purpose Quantum Mechanical Model, *J. Am. Chem. Soc. 107*, 3902−3909.
27. Rehse, P. H., Zhou, M., and Lin, S. X. (2002) Crystal structure of human dehydroepiandrosterone sulphotransferase in complex with substrate, *Biochem. J. 364*, 165−171.
28. Chang, H. J., Shi, R., Rehse, P., and Lin, S. X. (2004) Identifying androsterone (ADT) as a cognate substrate for human dehydroepiandrosterone sulfotransferase (DHEA-ST) important for steroid homeostasis: Structure of the enzyme-ADT complex, *J. Biol. Chem. 279*, 2689−2696.
29. Grishkovskaya, I., Avvakumov, G. V., Hammond, G. L., Catalano, M. G., and Muller, Y. A. (2002) Steroid ligands bind human sex hormone-binding globulin in specific orientations and produce distinct changes in protein conformation, *J. Biol. Chem. 277*, 32086−32093.
30. Ma, B., Shatsky, M., Wolfson, H. J., and Nussinov, R. (2002) Multiple diverse ligands binding at a single protein site: A matter of pre-existing populations, *Protein Sci. 11*, 184−197.

31. Ghosh, D., and Vihko, P. (2001) Molecular mechanisms of estrogen recognition and 17-keto reduction by human 17β-hydroxysteroid dehydrogenase 1, *Chem.-Biol. Interact. 130*−*132*, 637−650.
32. Nahoum, V., Gangloff, A., Shi, R., and Lin, S. X. (2003) How estrogen-specific proteins discriminate estrogens from androgens: A common steroid binding site architecture, *FASEB J. 17*, 1334−1336.
33. Apostolakis, J., Pluckthun, A., and Caflisch, A. (1998) Docking Small Ligands in Flexible Binding Sites, *J. Comput. Chem. 19*, 21−37.
34. Lange, G., Lesuisse, D., Deprez, P., Schoot, B., Loenze, P., Benard, D., Marquette, J. P., Broto, P., Sarubbi, E., and Mandine, E. (2002) Principles governing the binding of a class of non-peptidic inhibitors to the SH2 domain of src studied by X-ray analysis, *J. Med. Chem. 45*, 2915−2922.
35. Ferrari, S., Costi, P. M., and Wade, R. C. (2003) Inhibitor specificity via protein dynamics: Insights from the design of antibacterial agents targeted against thymidylate synthase, *Chem. Biol. 10*, 1183−1193.
36. Caflisch, A., Fischer, S., and Karplus, M. (1997) Docking by Monte-Carlo minimization with a solvation correction: application to an FKBP-substrate complex, *J. Comput. Chem. 18*, 723−743.
37. Cavasotto, C. N., Orry, A. J., and Abagyan, R. A. (2003) Structure-based identification of binding sites, native ligands and potential inhibitors for G-protein coupled receptors, *Proteins 51*, 423−433.
38. Tikhonov, D. B., and Zhorov, B. S. (2004) In silico activation of KcsA K^+ channel by lateral forces applied to the C-termini of inner helices, *Biophys. J. 87*, 1526−1536.
39. Nivon, L. G., and Shakhnovich, E. I. (2004) All-atom Monte Carlo simulation of GCAA RNA folding, *J. Mol. Biol. 344*, 29−45.

BI047553X